BL33XU
TOYOTA

1. Introduction

BL33XU, the Toyota beamline, was built in FY2009 and is operated by Toyota Central R&D Labs., Inc. [1]. The original purpose of this beamline was to perform quick-scanning X-ray absorption spectroscopy (QXAFS) for *operando* analysis and three-dimensional X-ray diffraction (3DXRD). These techniques were not available at SPring-8 before 2009 and were needed for industrial applications. In addition to these, the following techniques have been adopted: X-ray diffraction (XRD), X-ray computed tomography (CT)/laminography, and small-angle X-ray scattering (SAXS) as shown in Fig. 1. In this report, we describe the current status of this beamline and recent technical progress.

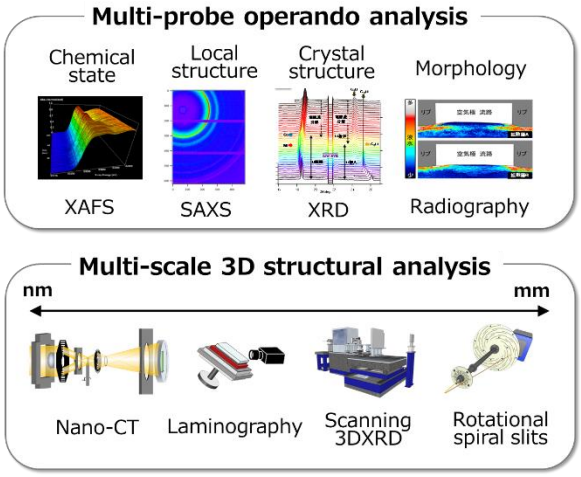

Fig. 1. Measurement techniques at BL33XU.

2. BL33XU beamline

2-1. Beamline layout

The medium-length BL33XU beamline has the optics hutch in the storage ring building of SPring-8. The experimental facility building is located outside the storage ring building. The building has three experimental hutches, a chemical laboratory, and an office room.

The layout of the optical components of BL33XU is shown in Fig. 2, where two different types of monochromator are installed. Optics 1 is mainly used for QXAFS. It is composed of horizontal deflection mirrors (M1 and M2) in the optics hutch, compact monochromators (C-Mono) with channel-cut crystals, and vertical deflection mirrors (M3 and M4) in experimental hutch 1. Optics 2 is used for 3DXRD and other techniques. It consists of a SPring-8 standard double-crystal monochromator, vertical deflection mirrors (M4 and M5), and Kirkpatrick–Baez focusing mirrors (KBMs) that yield a 1-μm-square microbeam at 50 keV in experimental hutch 3.

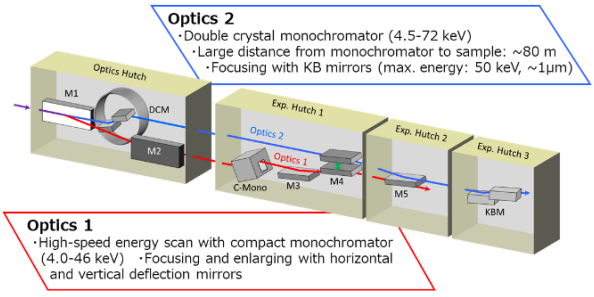

Fig. 2. Optical components of BL33XU.

2-2. Analysis techniques

(1) QXAFS

A tapered undulator combined with the servomotor-driven channel-cut monochromator realizes the rapid data acquisition of XAFS with a temporal resolution of 10 MS [2]. The energy range from 4.0 to 45 keV is accomplished by the two monochromators with Si(111) and Si(220) crystals.

This QXAFS system has enabled the development of various *in situ* measurement techniques such as simultaneous XAFS and XRD measurements of positive and negative electrodes of lithium-ion batteries during charging and discharging [3].

(2) SAXS

The camera distance from tens of centimeters to 4.5 meters can be selected for SAXS at BL33XU. A two-dimensional detector, PILATUS 300K (Dectris), is available for the developed *in situ* measurement system. An example is an *in situ* measurement system used to analyze the structural evolution of resins during the injection molding process [4].

(3) XRD

For the analysis of the reliability of mechanical and electronic components, it is important to measure the internal stresses and strains nondestructively. The measurement based on XRD was realized by a multi-axial goniometer equipped with a newly developed rotating and revolving spiral slit system. The rotating shield disks with the slits enable the detection of diffraction only from a small gage volume of interest inside a component with a two-dimensional detector, PILATUS. This system realizes the depth-resolved distribution measurement of strains in an actual mechanical component [5].

(4) Scanning 3DXRD

To measure the three-dimensional (3D) distribution of stresses inside the grains of a bulk sample, i.e., type III stresses, the scanning 3D X-ray diffraction (3DXRD) microscopy methodology was developed [6]. This nondestructive technique was validated in 2013 and the 3D distribution of stresses inside the grains of bulk polycrystalline steel under tensile deformation was measured in 2019 [7]. The results revealed that the microscopic intragranular stresses greatly deviate from the macroscopic average stresses measured by conventional methods. Combined with other nondestructive measurement techniques such as XRD and laminography, 3DXRD is expected to facilitate the development of multi-scale material modeling that expresses the deformation, fracture, and life of components.

(5) X-ray CT and laminography

To meet the growing need for the high-resolution nondestructive observation of internal behavior in mechanical and electronic components, X-ray computed tomography and laminography techniques were introduced. The resolutions of the two imaging techniques are less than 1 μm even under *in situ* measurement where sample materials and components are exposed to actual working conditions. The newly adopted CT system with a Fresnel zone plate (FZP) has achieved a resolution of ~100 nm.

3. Recent technological progress: Observation of water droplets in polymer electrolyte fuel cells (PEFCs) by X-ray computed nano-tomography

PEFC is one of the promising technologies for achieving carbon neutrality. To increase power density, it is important to manage liquid water that inhibits oxygen transport and electrochemical reactions in the cell. For example, when large amounts of liquid water accumulate in the GDL in layered PEFCs, oxygen transport is inhibited, resulting in a decrease in cell potential. The visualization of liquid water in PEFCs can contribute to strategies to avoid this phenomenon called flooding.

A microporous layer (MPL) is known to inhibit the flooding of PEFCs and to elucidate the

mechanism by which MPL inhibits flooding, it is also important to understand the accumulation and transport of water in the nanoscale pores of MPL. However, 3D observation techniques for simulation validation have not yet been realized. X-ray micro-CT has a limited spatial resolution, and it has not been possible to compare the simulation results with the experimental results of MPL. Therefore, we have established a computed nano-tomography (nano-CT) system using synchrotron radiation with a high spatial resolution of at least 200 nm and succeeded in observing liquid water in nanosized pores of MPL, the system of which is based on a full-field X-ray microscope and followed that of the BL47XU beamline at SPring-8. Details of the optical system are described elsewhere [8].

Two performance tests of the X-ray nano-CT system were conducted at the Toyota Beamline (BL33XU). One was a transmission image measurement of a test chart, and the other was a nano-CT measurement of a cut piece of MPL. X-ray nano-CT measurements were performed to visualize liquid water in MPL pores. Water vapor condensed in the air by cooling was used to provide liquid water in the pores. The incident X-ray energy was 8 keV. X-rays were monochromatized with a liquid-nitrogen-cooled Si (111) double-crystal monochromator, and high-order harmonic X-rays were reduced by a double total reflection Pt-coated mirror (5 mrad.) The illumination system of the X-ray microscope was a pseudo-Köhler illumination system with a rotating CZP. The exposure time of the X-ray projection image was 100 ms.

3D volume-rendered images of the entire field of view, measured by phase-contrast-mode X-ray nano-CT, were hierarchically classified into three categories: solid materials such as carbon black and PTFE, liquid water, and air voids. The solid materials ranged in size from a few hundred nanometers to a few micrometers, and some particles were agglomerated, while others were dispersed. The samples were porous structures with voids between the solid materials, and the porosity could be calculated. Liquid water was successfully observed as spherical droplets existing in the gaps between the porous materials.

Setoyama Daigo
Toyota Central R&D Labs., Inc.

References:

[1] Nonaka, T. et al. (2016). *AIP Conf. Proc.* **1741**, 030043.
[2] Nonaka, T. et al. (2012). *Rev. Sci. Instrum.* **83**, 083112.
[3] Makimura, Y. et al. (2016). *J. Electrochem. Soc.* **163**(7), A1450–A1456.
[4] Harada, M. et al. (2016). *SPring-8 User Experiment Report*, 2015A7003, 2015B7003.
[5] Setoyama, D. et al. (2015). *Proc. MECASENSE 2015*, 4.
[6] Hayashi, Y. et al. (2016). *SPring-8 User Experiment Report*, 2017A7002, 2017B7002.
[7] Hayashi, Y. et al. (2019). *Science* **366**, 1492–1496.
[8] Yamaguchi, S. et al. (2022). *J. Synchrotron Radiat.* **29(5)**, 1258–1264.